Automatic breathing phase identification based on the second derivative of the recorded lung sounds

Ravi Pal[a], Anna Barney[a]

[a] Institute of Sound and Vibration Research (ISVR), University of Southampton, Southampton, United Kingdom

***Abstract*— This paper presents a new method for automatic identification of the inspiratory and expiratory breathing phases in lung sound recordings. Adventitious lung sounds (wheezes and crackles), superimposed on the breath sounds, are generally an early indication of the disease, and their timing in the breathing cycle (early/mid/late inspiratory or expiratory) has clinical significance for monitoring or diagnosing disease. Therefore, the identification of the phases of the breathing cycle is an essential step for clinical interpretation of pulmonary auscultation. The proposed algorithm is designed to be robust in the presence of adventitious lung sounds or where the breath sounds may be noisy compared to heathy lung sounds. The algorithm uses the Savitzky & Golay (SG) filter to estimate the second derivative of the lung sound signal then calculates its normalized absolute value. A threshold value is used to clip any large amplitude peaks and, following low-pas filtering, the breathing phases are visible in the plotted signal. A rule-based approach based on identifying peaks and troughs is then used to identify inspirations and expirations. The performance of the method is evaluated using four different datasets: (a) a longitudinal dataset recorded from 19 subjects with a diagnosis of idiopathic pulmonary fibrosis (IPF), (b) cross-sectional dataset recorded from 55 subjects who were referred for high-resolution computed tomography (HRCT) scan of the chest for various clinical indications, (c) a longitudinal dataset recorded from 10 healthy subjects, and (d) an open access lung sounds dataset containing recordings from 41 subjects with wheeze (9 with chronic obstructive pulmonary fibrosis and 32 with asthma). On average for inspiratory phase identification the algorithm had a sensitivity of (mean (standard deviation)) 92.84 (12.88) %, positive predictive value of 90.64 (15.96) %, and F_1-score of 90.67 (12.53) %. For identification of the expiratory phase, the algorithm had an average sensitivity of 92.19 (13.44) %, an average positive predictive value of 91.55 (15.23) %, and an average F_1-score of 90.89 (12.45) %. The method shows good potential for automatic identification of breathing phases in recorded lung sounds.**

***Keywords*—Breathing cycle; Lung sounds; Breath phase identification.**

1. Introduction

In this paper we present an algorithm for automatic identification of the inspiratory and expiratory phases of the breathing cycle from a single-channel acoustic recording of the lung sounds. Each complete breathing cycle comprises an inspiratory phase followed by an expiratory phase. Within these phases lies important information for evaluating the health of the respiratory system, which can be located during inspiration or expiration [1]. Monitoring breathing patterns has critical importance in a wide range of clinical applications, including intensive care monitoring, anesthesia administration, rehabilitation, physiotherapy sessions and monitoring of sleep apnea as well as during cardiac and pulmonary examinations [1,2,3,4,5]. Abnormal breathing rates and changes in the breathing rate are among the earliest indicators of physiological instability.

Breathing rate (breaths per minute) and breathing phase (inspiration and expiration) can easily be identified using simple contact transducers [6, 7] and smartphone apps are now also available [8]. However, clinicians investigating cardio-vascular conditions are more used to manual auscultation by stethoscope and there are advantages to using adaptations to existing, trusted technology in terms of both efficiency during consultation and clinicians' willingness to adopt it [9]. We therefore present in this paper an algorithm for identifying the phases of the breath cycle from an acoustic recording of the lung sound acquired at a single location on the chest wall using a digital stethoscope.

During breathing, the air flowing into and out of the airways within the lungs generates sounds which can play an important role in assessing and monitoring cardiorespiratory patients [10]. These sounds can be divided into two different categories:

- breathing sounds, related to the flow of air through the airways are generally quiet, with expiration quieter than inspiration, but can become noisy in the presence of pathology [11]; and
- adventitious sounds of two main types: crackles and wheezes related to fluid-structure interactions between the airflow and the lung tissue [12].

These adventitious sounds are superimposed on the breath sounds and may alter the absolute or relative acoustic intensity of the inspiratory and expiratory breath phases, acting to mask the breathing sounds. Thus, classification of breathing phases from acoustic signals in the presence of adventitious sounds is especially challenging.

However, clinicians are interested not only in the presence or absence of adventitious sounds, but in their location within the breathing cycle [10, 13], whether inspiratory or expiratory and whether occurring early, mid, or late in that breathing phase. These timing factors can indicate the correct diagnosis, and changes in timing or an increase in the portion of the phase where added sounds are found can indicate disease progression.

Crackles, generally described as short, explosive, and non-musical in nature, may occur during inspiration or expiration, depending on the respiratory disease [14]. They are hypothesized to be due to the rapid opening or closing of small airways [15]. Wheezes are continuous (duration > 100 ms), more musical sounds [16] and may also occur in either breathing phase [17]. In clinical practice. pulmonary auscultation using a stethoscope is performed to assess lung health. This includes assessment for the presence of added lung

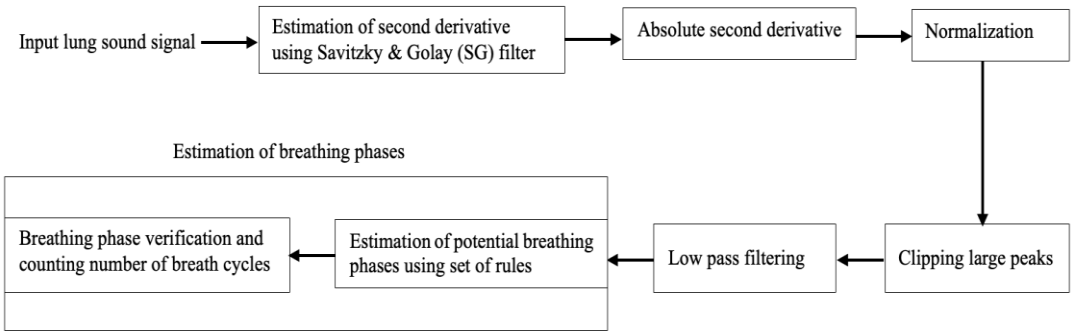

Fig. 1. Block diagram of the proposed algorithm for breathing phase identification.

sounds, and their timing within the breathing cycle (inspiratory or expiratory; early or late in the phase). The timing of crackles within the breathing cycle allows direct estimation of the origin of the sound [13]. Smaller airways have been shown to produce late inspiratory crackles of higher frequency and shorter duration (< 10 ms) known as fine crackles, whereas larger airways tend to produce crackles early in the inspiratory or expiratory phase with lower frequency and longer duration (> 10 ms) known as coarse crackles [10]. Fine crackles are associated with interstitial lung fibrosis, congestive heart failure, and pneumonia [18]; coarse crackles, are associated with chronic bronchitis, bronchiectasis, and chronic obstructive pulmonary disease (COPD) [19]. Moreover, in people with interstitial lung disorders the number of crackles per breath cycle (NOC/BC) is associated with the severity of the disease [20, 21]. The diseases most associated with wheeze are COPD and asthma [19]. Shim and Williams [17] have shown that in people with asthma, expiratory or inspiratory wheezing that has a combination of high pitch and moderate to severe intensity and that lasts the entire breathing phase is associated with a lower peak expiratory flow rate (a clinical measurement of airflow obstruction). The degree of bronchial obstruction in asthma is related to the proportion of the respiratory cycle the wheeze occupies [22] and wheezing in both breath phases has been associated with lower peak inspiratory flow rate than expiratory wheezing alone [17].

Lung sounds can be recorded using an electronic stethoscope and transferred to a computer for detailed analysis [23]. Many methods for detecting, isolating, and characterizing added lung sounds can be found in the literature [19] however, less emphasis has been given to automatic detection of breathing phases. In research studies, direct airflow measurement using a pneumotachograph is most common for estimating breathing phases [24]. The separate but simultaneous airflow measurements are used in conjunction with the sound recordings to estimate the timing of added sounds in relation to the breath phases. However, this approach demands a complex measurement set up, and hence is not suitable for use in clinical practice [25]. In the absence of information about flow direction, the audio-visual marking of breathing phases on recorded lung sound files is both time consuming and subjective. Thus, a reliable, objective, and automated method for breath phase identification from recorded lung sounds alone. without the need for either pneumotachograph or audio-visual marking would offer advantages in clinical and research evaluation of recorded lung sounds.

Several studies have been reported which use a transducer at the tracheal notch to detect breath phase, with analysis based on acoustical means [5,26,27,28]. The breath phase detection accuracy of these methods lies in the range of 93 % to 100 %. However, although, these methods have high accuracy, they are dependent on recording of the tracheal sounds where breath sound is loud, and phase can be easily distinguished acoustically [29]. In clinical practice tracheal sounds are generally used to assess the status of the upper airways [29] whereas for cardio-respiratory analysis it is typically the sounds measured on the chest wall that are of interest, and simultaneous measurement using multi-channel devices in more than one location may be impractical. Unlike tracheal sounds, breath sounds measured on the chest wall are quieter, especially in the expiratory phase. Furthermore, these published methods were validated (except [5]) using lung sounds recorded from healthy subjects and their detection accuracy was not tested on lung sounds recorded from subjects with respiratory diseases. where adventitious sounds may dominate [30,31]. Therefore, it is possible that these methods may be less accurate when applied to lung sounds recorded from subjects with respiratory disease [25].

More recently, methods have been presented to address some of the limitations mentioned above. Messner et al. [32] used a bidirectional gated recurrent neural network (BIGRNNs). This method was tested on lung sounds recorded from healthy subjects and on subjects with IPF and achieved an overall performance assessed via the F_1-score of 85.5 %. Jacome et al. [25] proposed a convolutional neural network with a spectrogram-based method. Its performance was validated on lung sounds recorded from subjects with and without respiratory disease. They found an average sensitivity of 97 % and an average specificity of 84 % for identifying the breathing phases. Mclane et al. [33] proposed a system, using a collection of new methods together with robustness-focused improvements on previous methods to estimate breathing cycle location and to detect pulmonary crackles. The method was validated using simulated lung sounds and a small set of real lung sounds (20 recordings) recorded from healthy subjects and subjects with cystic fibrosis. For breathing phase detection, this method had an average F_1-score of 94.43 %. All three methods performed well, but it is important to notice that all three methods utilize deep learning processes and as mentioned in [25] a common problem with machine learning methods is that they often work well with a generated dataset with samples recorded in an identical manner for both training and testing

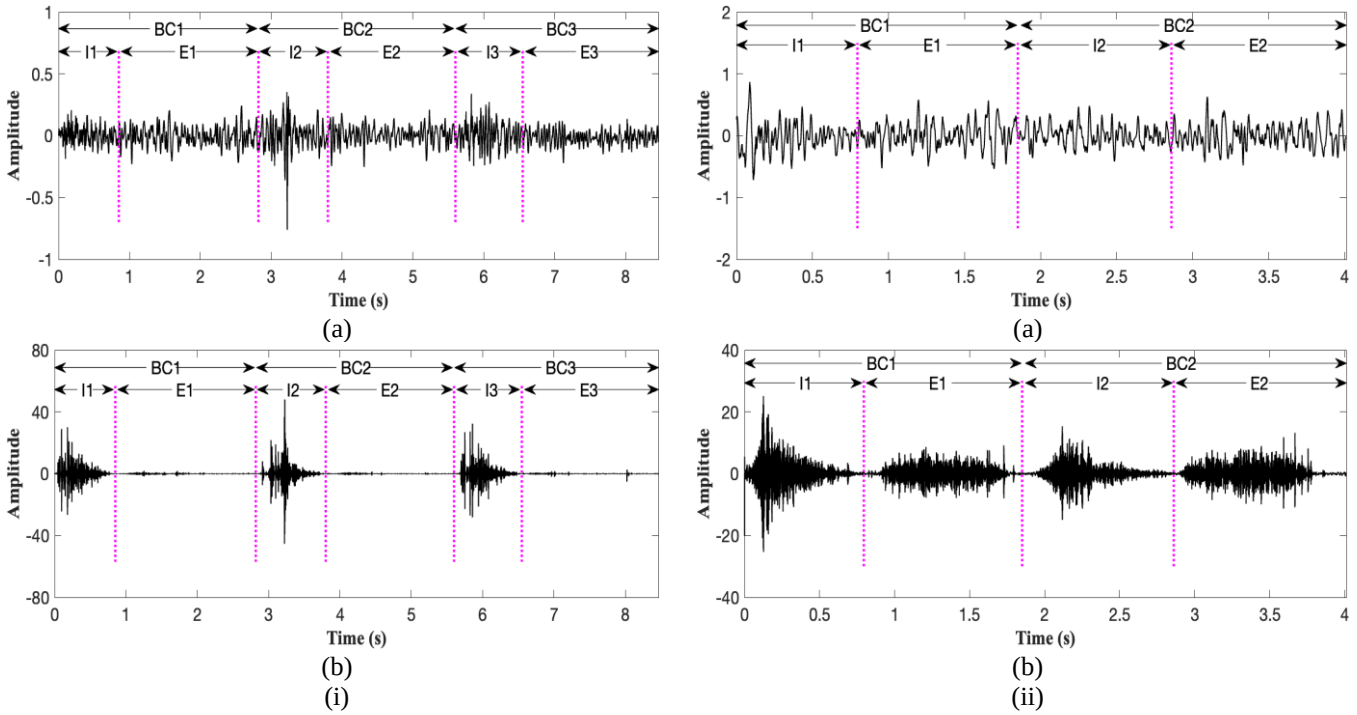

Fig. 2. Input lung sound signals selected from the longitudinal dataset recorded from IPF subjects; (i): - (a) Input lung sound signal (measured on the posterior right lung base (at 5 cm from the paravertebral line and 7 cm below the scapular angle) (b) Estimated second derivative of the input lung sound signal. (ii): - (a) Input lung sound signal (recorded on the posterior left chest wall at apex (2 cm from the paravertebral line, in one of the first intercostal spaces) (b) Estimated second derivative of the input lung sound signal. I: Inspiratory phase; E: Expiratory phase; BC: Breath cycle. The pink, vertical dotted lines show the boundaries of the audio-visually marked breathing phases.

sets but may not perform as well when applied to new unseen datasets. Bandyopadhyaya et al. [34] recently introduced an envelope-based approach for detecting breathing phases. This method was evaluated using lung sounds from both healthy subjects and those with respiratory diseases. The method had an average accuracy of 94.61% for normal subjects and 91.98% for disease cases. However, the test dataset was fairly small (88 subjects, each with a single recording) and while four different pathological conditions were included, there were fewer than 40 subjects per condition. Although they report that the presence of adventitious sounds may be expected to raise the dominant frequency range of the lung sounds to above 200 Hz, the authors provide confirmation that adventitious sounds were present in the test signals.

Other methods for detecting breathing phases, such as a fuzzy inference system [1] and an adaptive neuro-fuzzy inference system [4], have also been proposed. They considered both tracheal as well as basal lung sounds. These methods were evaluated using a correlation coefficient and the root mean square error (RMSE). The fuzzy inference system had a correlation coefficients of r = 0.9892 and r = 0.9964 for Mamdani- and Sugeno-type fuzzy inference systems, respectively, with corresponding RMSE values of RMSE = 0.0853 for Mamdani and RMSE = 0.0817 for Sugeno. The adaptive neuro-fuzzy inference system had a correlation coefficient of r = 0.9925 and an RMSE of 0.0069. Despite the good results, the dependency of these methods on a supervised learning strategy may limit their generalization as these methods can be biased towards a specific database [34]. Moreover, the computational cost of an adaptive neuro-fuzzy inference system is high due to its complex structure and gradient learning [35].

In this paper, we present a new signal processing algorithm for automatic breathing phase identification in recorded lung sounds. We aimed to develop a method that is robust for lung sounds recorded from subjects with and without respiratory disease, therefore the algorithm is validated using four different datasets, a longitudinal dataset recorded from IPF subjects, a cross-sectional dataset of subjects with a range of suspected pulmonary diseases who had been referred for an HRCT scan, a longitudinal dataset recorded from healthy subjects, and an open access dataset with wheezes recorded from subjects with COPD and Asthma [36].

The rest of the paper is arranged as follows; section 2 describes the detailed working process of the proposed method. Section 3 presents the datasets and the quantitative evaluators used to assess the outcome of the method. The experimental results are presented in Section 4. Section 5 presents the discussion of the results and Section 6 concludes the work.

2. An automatic algorithm for breathing phase identification

In healthy subjects, the breathing phases are predominantly related to the higher intensity parts of the audio signal, which will retain large amplitude in the signal's second derivative,

whereas only the residue of coefficients related to quieter parts will be preserved. The (absolute) value of the second derivative may vary significantly in amplitude between recording locations and subjects, therefore in this study, its value is normalized to an amplitude range of 0 to 1 for further processing. Large amplitude peaks in the signal may be due to adventitious sounds such as crackles, movement artefact, heart sounds etc, and may confound the automated identification of the breathing phases. Therefore, once the normalized absolute second derivative is calculated, the large amplitude peaks are clipped using a threshold value estimated from the signal statistics. The processed signal is then low pass filtered and the breathing phases are identified. The algorithm therefore consists of five steps: (1) Estimation of second derivative, (2) normalization, (3) clipping large peaks, (4) low pass filtering, and (5) identification of breathing phases, which are described in detail in the following sections. For clarity, the steps of the algorithm are shown schematically in Fig. 1.

2.1. Estimation of second derivative

The second derivative of the input signal is calculated using a Savitzky & Golay (SG) filter [37]. The SG filter parameters are degree of fitting polynomial p_f = 4, number of coefficients $n_c = 89$; order of derivation d_o = 0, 1 and 2 for smoothing the lung sound signal, and estimating first and second derivative of the smoothed lung sound signal respectively [38]. The SG filter is used for calculating the second derivative because it generates the second derivative from a smoothed version of the input signal. As an example: two cases are shown in Fig. 2 (i) and Fig. 2 (ii) in which inspiratory phases, expiratory phases, and breath cycles have been audio visually marked by an experienced pulmonary acoustics researcher using open access Audacity software. Fig. 2 (i-a) shows an input lung sound signal selected from the longitudinal dataset recorded in IPF subjects, the lung sound was measured on the posterior right lung base (at 5 cm from the paravertebral line and 7 cm below the scapular angle) for which the inspiratory phases have slightly higher rms amplitude on average (0.084 normalized arbitrary units) than the expiratory phases (0.068). From Fig. 2 (i-b), it can be seen that the coefficients related to the inspiratory phases retain large amplitude in the second derivative, whereas the coefficients corresponding to the quieter, expiratory phases are smaller in amplitude. In another example, Fig. 2 (ii- a) shows an input lung sound signal selected from the longitudinal dataset recorded from IPF subjects, recorded on the posterior left chest wall at apex (2 cm from the paravertebral line, in one of the first intercostal spaces) in which both inspiratory and expiratory phases are of similar rms amplitude. On average, the RMS amplitude of the inspiratory phases is 0.192, while that of the expiratory phases is 0.190. In the second derivative, shown in Fig. 2 (ii-b), it is clear that when both phases have similar rms amplitude, the coefficients related to both phases also have similar rms amplitude in the second derivative.

The second derivative of an input lung sound signal estimated using SG filter may more clearly reveal inspiratory and expiratory phases than the raw lung sound recording, but it does not alone automatically identify inspiratory and expiratory phases.

2.2. Estimation of absolute value of second derivative and normalised absolute value of second derivative

Next the absolute value of the second derivative signal is calculated. The input lung sound signal, its second derivative, and the absolute value of its second derivative are shown in Figs. 3 (a), (b), and (c), respectively, with the inspiratory phases, expiratory phases, and breath cycles marked by arrows. The absolute value of the second derivative may vary significantly, in amplitude between recording locations and subjects, therefore, its value is normalized to an amplitude range of 0 to 1 using Eq. 1. Let $|s''(n)|$ be the absolute value of the second derivative of the smoothed lung sound signal with respect to time, where n is the sample index. Then the normalised absolute value of the second derivative is given by:

$$|s''(n)|_{norm} = \frac{|s''(n)| - |s''(n)|_{min}}{|s''(n)|_{max} - |s''(n)|_{min}} \quad (1)$$

where $|s''(n)|_{min}$ is the minimum of the absolute value of the second derivative, and $|s''(n)|_{max}$ is its maximum value. The normalized absolute second derivative is shown in Fig. 3 (d).

2.3. Clipping large amplitude peaks from the normalized absolute second derivative

Large amplitude peaks in the lung sound signal may be due to adventitious sounds such as crackles, movement artefact, heart sounds etc. and may confound the automated identification of the breathing phases. Therefore, peaks in the normalized absolute second derivative larger than a defined threshold are clipped. A suitable threshold value for each signal is determined, based on [39], from the frequency histogram plot of the normalized absolute second derivative as: the value having on its left, 80 % of total area under the curve. The frequency histogram plot of the normalized absolute second derivative is shown in Fig. 3 (e). Fig. 3 (f) shows the normalized absolute second derivative after clipping the large amplitude peaks.

2.4. Low pass filter

The clipped normalized absolute second derivative is passed through a 3rd order Butterworth low pass filter with cut off frequency of either 2.5 Hz or 1 Hz. Usually, a person with cardiorespiratory disease breathes faster than a healthy subject. Therefore, the higher cut off frequency: 2.5 Hz, is selected for the IPF longitudinal, cross-sectional, and the open access datasets and the lower cut-off frequency: 1 Hz, is selected for healthy subjects. Here, the cut off frequencies 2.5 Hz and 1 Hz are empirically selected. Fig. 3 (g) shows the output of the low pass filter.

2.5. Identification of breathing phases

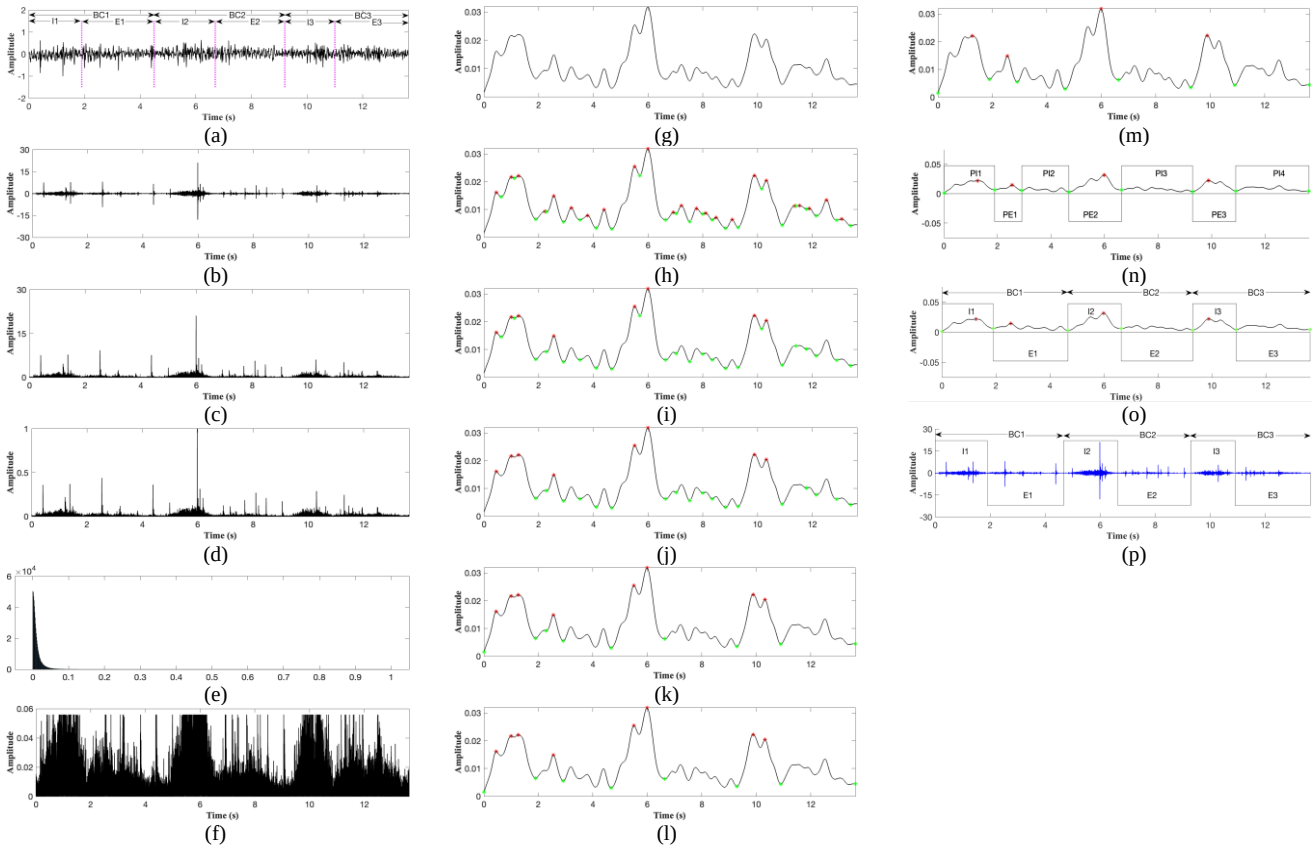

Fig. 3: (a) Input lung sound signal with (vertical dotted lines) audio-visually marked breath phases; (b) Second derivative of the input lung sound signal; (c) Absolute value of the second derivative; (d) Normalized absolute second derivative; (e) Frequency histogram of the normalized absolute second derivative; (f) Clipped normalized absolute second derivative; (g) Low pass filter output; (h-m) Low pass filter output with different conditions of the filter (see section 2.5); (n) Low pass filter output with potential inspiratory phases and expiratory phases; (o) Low pass filter output with verified breathing phases and breathing cycles; (p) Second derivative of the input lung sound signal with verified breathing phases and breath cycles. I: Inspiratory phase; E: Expiratory phase; BC: Breath cycle.

This step is divided into two sub steps**:** An initial identification of breathing phases (potential breathing phases) is made using a set of rules defined in section 2.5.1 (i-vi) and this is then refined using a calculated threshold (Eq. 2) to give a final labelling of the breathing phases as either inspiration or expiration.

2.5.1 Identification of potential breathing phases

In this step, a set of rules based on the peaks and valleys of the low pass filter output are used to search for potential breathing phases [40]. Peaks are candidates to be considered as points of greatest airflow in or out (approximately the middle of a breath phase) and valleys are candidates for the change from one phase to the other. Fig. 3 (h) shows all identified peaks and valleys of the low pass filter output, where peaks are shown using red stars and valleys are displayed using green stars. The following set of rules are used in this step:

(i) Peaks of the low pass filter output which are 0.5 standard deviations above the mean amplitude of the low pass filter output are identified (see Fig. 3 (i)).

(ii) Valleys of the low pass filter output which are less than the mean amplitude of the low pass filter output are identified (see Fig. 3 (j)).

(iii) Of the valleys identified in (ii), only the valley immediately before and immediately after each peak is considered. If there is no identified valley before the first peak, then the first sample of the signal is used and correspondingly if there is no valley after the final peak the last sample of the signal is used. (See Fig. 3 (k)).

(iv) As mentioned in [26], the average duration of a breathing phase is approximately 1 s. Therefore, the distance between an estimated peak and the closest estimated valley, is expected to be of the order of 500 ms on average and the distance between any two estimated valleys is expected to be of the order of 1 s. Valleys which are closer to a peak than 200 ms are therefore discarded, with the choice of proximity measure being made to allow for breath-to-breath variation in cycle duration.

(v) Next, any valley which is less than 500 ms from a previous valley, it is discarded from the analysis. As an example, see Fig. 3 (l), where the valley just after 2

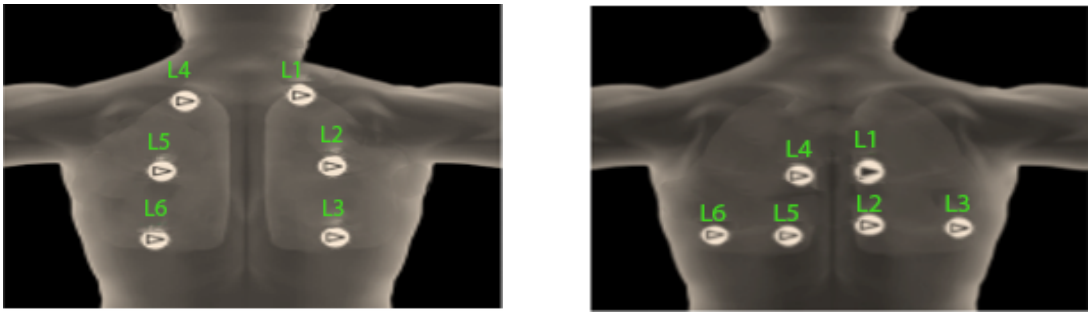

(a) (b)

Fig. 4: (a) Data recording sites for the longitudinal dataset recorded from IPF subjects and longitudinal dataset recorded from healthy subjects (L1-L6), (b) Cross-sectional dataset lung sounds recording sites (L-L6).

s in Fig. 3 (k) is discarded (compare with Fig. 3 (l)). Note that once any valley is discarded then it is not used for comparing with other valleys.

(vi) If more than one peak exists between two valleys, only the biggest peak amongst them is considered, with the others being discarded (compare Figs. 3 (l) and (m).

(vii) Next the remaining valleys are connected together using alternating positive and negative cycles of a square wave always starting with a positive cycle (see Fig. 3 (n)). Complete breathing cycles are typically considered to start with inspiration and the assumption at this stage of the analysis is that the first cycle identified is inspiratory. This can be corrected in the next step if the assumption proves to be incorrect.

Note that the threshold values in rules i) and iv) were selected based on the proposals in [26].

2.5.2 Breathing phase verification and counting number of breath cycles

Usually, in lung sounds recorded from posterior chest locations, the amplitude of the inspiratory phases is much greater than of the expiratory peaks [41,42]. Therefore, as a last step, peak values for potential inspiratory phases are compared to a threshold, defined by:

$$\vartheta_p = \frac{\mu_{p(k)}}{2} + \sigma_{p(k)} \quad (2)$$

Where ϑ_p is called the peak threshold, and $\mu_{p(k)}$and $\sigma_{p(k)}$ are, respectively, the average and standard deviation of the amplitudes $p(n)$ of the remaining k peaks after step (vi) in section 2.5.1.

We denote the process of comparing the amplitude of the potential inspiratory peaks to the peak threshold as breathing phase verification. The verification process starts with the first potential inspiratory phase. If the first potential inspiratory phase has a peak with an amplitude greater than the peak threshold, it is considered as a true inspiratory phase and verification moves to the next potential inspiratory phase. During the verification process if any potential inspiratory phase (including the first potential inspiratory phase) does not have a peak or has a peak with an amplitude less than or equal to the peak threshold, the first valley before that potential inspiratory phase is disregarded. Then, the remaining valleys are reconnected with each other using a new square wave (starting with a positive cycle) retaining any previously verified inspiratory phases and redefining any potential inspiratory phases for subsequent verification. Verified expiratory phases are indicated by the negative going square wave cycles between verified inspirations, negative square wave cycles between potential inspiration cycles are potential expirations. Following reconnection, the verification process then continues with the next potential inspiratory phase.

The verification process ends when all positive square wave cycles contain a peak with amplitude greater than the peak threshold. At the end of the process all positive cycles with peaks greater than the peak threshold are considered verified inspiratory phases and all negative rectangles with or without peaks are considered verified expiratory phases.

Based on the verified breathing phases the number of complete breath cycles is calculated. The combination of two phases one identified as inspiratory and one as expiratory (starting with an inspiratory phase) makes up one breath cycle and the total of all such combinations represents the number of breath cycles.

The verified inspiratory and expiratory phases plotted on the low pass filtered signal are shown in Fig. 3 (o) using positive and negative square wave cycles respectively. Additionally, arrows at the top of the plot indicate the whole breath cycles. The same verified inspiratory and expiratory phases together with the breath cycles are displayed again in Fig. 3 (p) plotted against the second derivative of the input lung sound signal. Visual comparison of the automatic identification results (Fig. 3 (o or p)) with the audio-visual marking (Fig. 3 (a)) shows the same number of inspiration and expiration phases in both, with closely comparable breath phase boundaries.

3. Test datasets and performance evaluators

3.1. Datasets Description

The algorithm is validated using four different lung sound datasets: (a) a longitudinal dataset recorded from 19 subjects with a clinical diagnosis of IPF, typically characterized by the

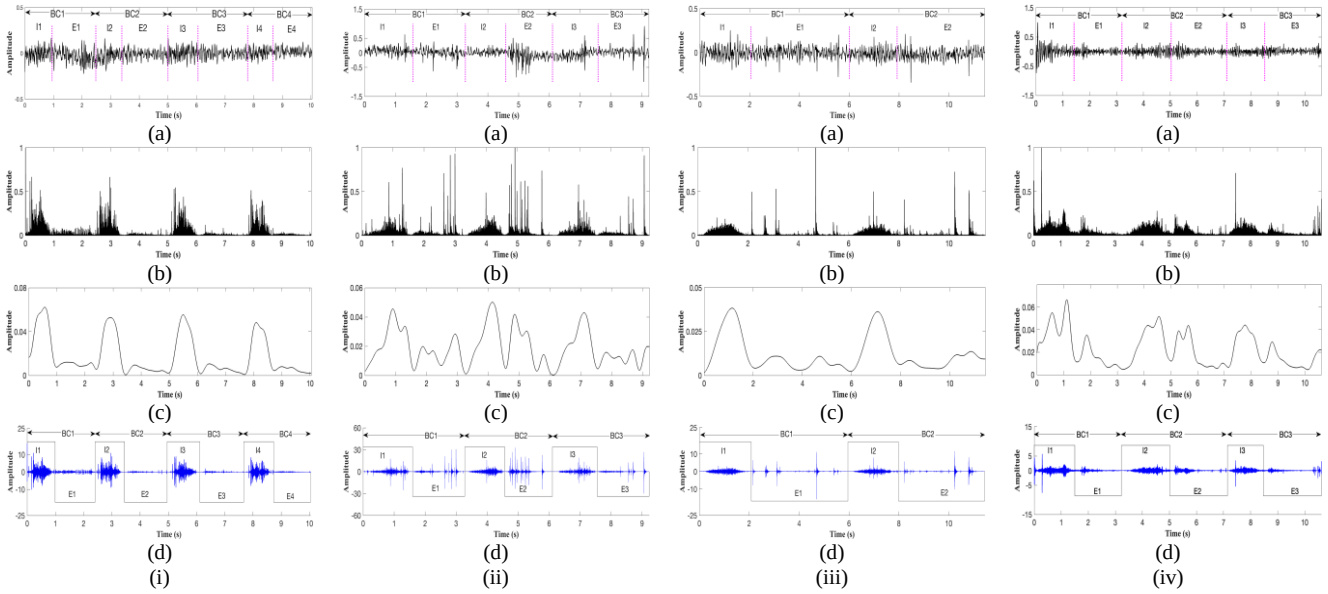

Fig. 5: (i) (a) Input lung sound signal selected from the longitudinal dataset recorded from IPF subjects ; (b) Normalized absolute second derivative; (c) Low pass filter output; (d) Second derivative of the input lung sound signal with verified breathing phases and breath cycles; (ii) (a) Input lung sound signal selected from the cross-sectional dataset; (b) Normalized absolute second derivative; (c) Low pass filter output; (d) Second derivative of the input lung sound signal with verified breathing phases and breath cycles; (iii) (a) Input lung sound signal selected from the longitudinal dataset recorded from healthy subjects; (b) Normalized absolute second derivative; (c) Low pass filter output; (d) Second derivative of the input lung sound signal with verified breathing phases and breath cycles; and (iv) (a) Input lung sound signal selected from the open access dataset recorded from asthma and COPD subjects containing wheezes [36]; (b) Normalized absolute second derivative; (c) Low pass filter output; (d) Second derivative of the input lung sound signal with verified breathing phases and breath cycles. I: Inspiratory phase; E: Expiratory phase; BC: Breath cycle.

presence of fine crackles, (b)) a longitudinal dataset recorded from 10 healthy subjects, (c) a cross-sectional dataset recorded from 55 subjects who were referred for HRCT scan of the chest for various clinical indications of possible pulmonary disease, including IPF. These are likely to have fine or coarse crackles, wheeze or noisy breath sounds (eventual diagnosis for the subjects is not known), and (d) an open access lung sound dataset containing 41 recordings with wheeze (9 subjects with a diagnosis of COPD and 32 subjects with a diagnosis of asthma) [36]. The subjects for the longitudinal dataset (IPF and healthy groups) were recruited in the University Hospital of Southampton, UK between March and September 2015. The subjects for the cross-sectional dataset were recruited in the Radiology Units of the University Hospitals of Modena in Italy [43]. All data used in this study was robustly anonymised and no identifying information or personal data was available to the researchers. Prior to use of the data, it was confirmed that all contributary studies had independent approval by a relevant ethics committee, involved the use of appropriate signed, informed consent prior to data collection and conformed to the Declaration of Helsinki (1964) and its successive revisions. The data used was a convenience sample drawn from available sources designed to determine how the analysis performed over a set of samples that were heterogeneous in terms of subject demographics, health status, nature of adventitious sounds, recoding environment and recording conditions (e.g., sampling frequency, stethoscope filter settings, recording duration etc).

In both longitudinal datasets (IPF and healthy subjects), each subject's lung sounds were recorded over 7 visits (each visit approximately 2 months apart) over a one-year period. For the cross-sectional database a single set of recordings was made for each subject. In each of these three datasets the lung sounds were recorded at 6 posterior locations using an electronic stethoscope (Littmann 3200; 3M, St. Paul, MN, USA). Fig. 4 (a) shows the 6 posteriors lung sound recording locations for the two longitudinal datasets and Fig. 4 (b) indicates the 6 posterior locations (L1-L6) of the cross-sectional dataset. The open access dataset was recorded, also using the model 3200 3M Littmann Electronic stethoscope, at the King Abdullah University Hospital, Jordan [36] at a single chest location per subject. This dataset was predominantly recorded from posterior locations on the chest wall (14 at the base, 11 over the upper lung and 11 midway between upper and lower), with five recordings on the anterior chest wall (2 at the base, 2 over the upper lung and 1 midway between upper and lower). Note that to test the breathing phase identification of our method in the presence of wheezes, we included in this study only the recordings with identified wheeze from the larger dataset available. The selected recordings were made using the extended mode filtration of the 3M Littmann Electronic Stethoscope Model 3200. We refer readers to [36] for a more detailed description of the open access dataset.

In the IPF longitudinal dataset out of 19 IPF subjects 13 completed the total 7 visits with one lung sound recording per visit at each of 6 posterior locations. 2 subjects withdrew from the study due to poor health and 3 subjects died during the

observation period [43]. One subject completed the total 7 visits but missed one lung sound recording at location L1 (see Fig. 4 (a)) in one of the 7 visits. Therefore, in the IPF longitudinal dataset, in total 689 lung sound files were analysed. In the healthy subject longitudinal dataset, out of 10 subjects 7 completed the study. 3 withdrew from the study at some point due to personal or otherwise non-specified reasons [43]. From 7 subjects, 6 completed the total 7 visits and 1 skipped a visit during the observation period. Therefore, in the healthy subject longitudinal dataset, out of 336 lung sound files, 282 lung sound files were analysed. 54 lung sound files were excluded from the study due to inaudibility of breathing phases or breath cycles which prevented reliable audio-visual marking of the breathing cycles. In the cross-sectional dataset out of 300 available lung sound samples recorded from 55 subjects, 258 lung sound files were analysed. 42 lung sound files were excluded, again due to inaudible recordings preventing manual file mark-up. In the open access dataset out of 41 recordings from 41 subjects with wheezes 34 lung sounds files were used for the analysis. 7 lung sound files were excluded due to the inaudibility of breathing phases or breath cycles.

In all four datasets, each lung sound file was marked audio-visually by an experienced pulmonary acoustics researcher using open access Audacity software to indicate the number of inspiratory phases, number of expiratory phases, and number of breathing cycles. These marked up signals served as a reference for the evaluation of the algorithm. In each lung sound file only full breathing cycles (inspiratory phase followed by an expiratory phase) were counted. In a smaller number of files, the location of the start and end of each breathing phase was also marked using audio-visual prompts and these landmarks are indicated by the horizontal arrows in Fig. 5. However, this more detailed process was time-consuming, and the start and end of a breathing phase is hard to define systematically, so it was undertaken only for a subset of the files likely to be used in figures. In general, therefore, evaluation determines the frequency with which the correct number of inspirations and expirations are identified in a sample, but the accuracy of prediction of the start and end of each cycle has not been systematically tested in this study and hence nor has an estimate of breathing cycle duration. The different lung sound datasets used for evaluating the performance of the algorithm are shown in Table 1.

Table 1
Lung sound datasets used for evaluating the algorithm.

Dataset	Number of lung sound files	Number of complete breath cycles marked audio-visually
IPF longitudinal dataset	689	2416
Healthy subjects' longitudinal dataset	282	905
Cross-sectional dataset	258	741
Open access dataset	34	197

3.2. Performance evaluators

Three metrics are used for evaluating the breathing phase identification performance of the algorithm: sensitivity (SE), positive predictive value (PPV), and F_1-score (F_1). These metrics compare the automatic method results with audio-visual marking by an experienced pulmonary acoustic researcher (ground truth) in terms of the number of occurrences of each breathing phase. SE is the fraction of true (i.e. audio-visually marked) inspiratory (or expiratory) phases identified by the algorithm; PPV is the fraction of cycles assigned as inspiratory (or expiratory) by the algorithm which are true inspiratory (or expiratory) cycles, and F_1-score is the harmonic mean of SE and PPV [44], commonly interpreted as a measure of the overall performance of a classification system, which ranges from 0 to 1 with higher values indicating better performance.

$$SE = \frac{number\ of\ true\ ins.(or\ exp.)\ phases\ detected}{number\ of\ true\ ins.(or\ exp.)\ phases} \quad (3)$$

$$PPV = \frac{number\ of\ true\ ins.(or\ exp.)\ phases\ detected}{number\ of\ ins.(or\ exp.)\ phases\ detected} \quad (4)$$

$$F_1 = 2 \times \frac{SE \times PPV}{SE + PPV} \quad (5)$$

These three metrics were also used for evaluating the performance of the algorithm when calculating the number of entire breath cycles identified.

4. Experimental results

The performance of the algorithm for identifying breathing phases, and for calculating the number of breath cycles in each recording is presented in Tables 2 and 3, respectively in terms of the SE, PPV, and F_1-score for each data set (results are reported as mean (standard deviation) of the SE, PPV, and F_1-score presented as a percentage).

To illustrate the performance of the algorithm on each dataset, Fig. 5 shows one example from each of the four datasets. Plots labelled (a) show the input lung sound signal with breathing phases and number of breath cycles audio-visually marked, plots labelled (b) show curves for the normalized absolute second derivative signals, plots labelled (c) show curves for the low pass filter outputs, plots labelled (d) show curves for the second derivative of the input lung sound signals with verified breathing phases and number of breath cycles where positive square wave cycles show the verified inspiratory phases, negative square wave cycles indicate the verified expiratory phases, and the combination of one inspiratory phase followed by one expiratory phase represents a breath cycle. Comparison of the number of each type of breathing phase and the number of breath cycles identified using the algorithm (plots labelled (d)) with those marked audio-visually on the input lung sound signal (plots labelled (a)) shows that the number of breathing phases and the number of

Table 2
Sensitivity, Positive predictive value, and F_1-score for number of inspiratory phases, expiratory phases, and both phases (results are reported as mean (standard deviation) of the percentage of SE, PPV, and F_1).

	Inspiratory phases			Expiratory phases			Both inspiratory and expiratory phases		
Dataset	SE %	PPV %	F_1 %	SE %	PPV %	F_1 %	SE %	PPV %	F_1 %
IPF longitudinal dataset	93.31 (12.73)	91.11 (15.63)	91.27 (12.53)	92.93 (13.14)	91.74 (15.07)	91.45 (12.44)	93.12 (12.79)	91.43 (15.23)	91.36 (12.43)
Cross-sectional dataset	96.61 (9.71)	90.13 (17.73)	92.28 (13.18)	95.38 (11.31)	91.45 (16.64)	92.59 (13.21)	95.99 (9.97)	90.79 (16.90)	92.43 (12.99)
Healthy subjects' longitudinal dataset	88.96 (14.35)	90.29 (15.12)	88.19 (11.33)	88.22 (14.71)	91.32 (14.43)	88.37 (11.27)	88.59 (14.30)	90.80 (14.62)	88.28 (11.13)
Open access dataset [36]	86.78 (14.18)	87.90 (15.40)	86.94 (13.70)	85.80 (14.34)	90.17 (14.02)	87.46 (12.78)	86.29 (14.07)	89.03 (14.39)	87.20 (13.06)
Average	92.84 (12.88)	90.64 (15.96)	90.67 (12.53)	92.19 (13.44)	91.55 (15.23)	90.89 (12.45)	92.51 (12.93)	91.09 (15.42)	90.78 (12.37)

Table 3
Sensitivity, Positive predictive value, and F_1-score for number of breath cycles (results are reported as mean (standard deviation) of the percentage of SE, PPV, and F_1).

Dataset	SE %	PPV %	F_1 %
IPF longitudinal dataset	95.95 (10.35)	94.52 (12.68)	94.27 (9.27)
Cross-sectional dataset	98.47 (6.16)	94.50 (14.11)	95.63 (9.56)
Healthy subjects' longitudinal dataset	91.23 (13.82)	94.36 (12.95)	91.37 (9.99)
Open access dataset [36]	92.95 (10.46)	97.39 (6.68)	94.59 (6.17)
Average	95.33 (10.85)	94.56 (12.92)	93.91 (9.53)

breath cycles are correctly identified by the algorithm.

In most of the files in the datasets only a count of the number of each type of breathing phase was made. However, the files used for comparison in the plots in Fig. 5 are taken from the small sample where the location of start and end of each breathing phase was also systemically identified by audio-visual means. For this sub-set of the data, it was verified that the automatic detection of the start and end of the breathing phase by the algorithm was within 0.5 s of the locations found by audio-visual marking. This error tolerance is the same as the criterion used in [33] suggesting that the algorithm could also be valid if used to estimate the duration of each phase and its beginning and end points, but this remains to be tested.

5. Discussion

We have presented a novel breathing phase identification algorithm based on the second derivative of lung sounds recorded on the chest wall with an electronic stethoscope. Lung sound characteristics may vary with the health status of the subject and the location on the chest where the recording is made. Jacome et al. [25], note that systems designed to detect breathing phases should be tested using lung sounds recorded at different chest locations and on large datasets recorded from subjects with and without cardiorespiratory disease. Therefore, in this study we have validated our method on lung sounds recorded from both healthy and cardiorespiratory subjects with a range of different clinical indicators conditions. Our longitudinal data sets include subjects at different stages of disease progression.

Table 4 compares the performance of the new method with previously published methods. We note that our system can identify breathing phases from breathing sounds only, whereas [26], [5], [27], and [28] all use recordings of tracheal sounds not normally acquired during clinical auscultation. Breathing sounds are generally quieter than tracheal sounds, especially during expiration, are more variable and more prone to masking by noise, The primary focus of our performance comparison is therefore on systems using breathing sounds only [25, 32, 33, 34]. The performance of our signal processing-based method is compared with two deep learning methods: In comparison with the bidirectional gated recurrent neural networks (BIGRNNs) method [32] (F_1-score (mean) = 85.5 %), the proposed method showed higher overall performance (F_1-score (mean (standard deviation)) = 90.78 (12.37) %). The convolutional neural network with a spectrogram-based method [25] showed high average SE (97 %) but at the cost of low average specificity (84 %), whereas our method has demonstrated overall balanced results (SE = 92.51 (12.93) %, PPV = 91.09 (15.42) %, and F_1-score = 90.78 (12.37) %; where results are shown as mean (standard deviation)). We also compare with the robustness focused system presented by Mclane et al. [33] which uses a neural network to denoise the signals but adopts a signal processing approach for breath cycle detection. Their system has slightly higher performance than our method, though we note that their validation was largely based on simulated lung sounds, with a real subject test set of only 20 recordings (14 subjects of which 5 were healthy, 140 breathing cycles). Additionally, their primary interest was signals containing crackles, with no wheeze samples reported in their test data set. In comparison our method is validated on 1263 real lung sound recordings obtained in a clinical setting. In vivo recordings have different characteristics to simulated recordings [33], therefore the system introduced by Mclane et al. [33] remains to be fully tested on a large, heterogeneous dataset recorded from real

Table 4
Summary of the proposed and established methods breathing phase detection results with their real lung sounds evaluation settings.

	Subjects for evaluation		Real lung sound recordings (number)	Results in terms of SE, PPV or Specificity, F_1-score, or Accuracy (Values are displayed as mean (standard deviation)/ Where standard deviation is not available only the mean value is shown)
	Healthy (number)	Respiratory condition (number)		
Breathing sounds (recorded from various chest locations) dependent methods				
Proposed method	10	115	1263	SE=92.51 (12.93) %, PPV= 91.09 (15.42) %, and F_1-score= 90.78 (12.37) %
Mclane et al. [33]	5	9	20	SE= 94.4 %, PPV= 97.7 %, and F_1-score= 96.1 %
Jacome et al. [25]	6	14	>1200	SE= 97 % and Specificity= 84 %
Messner et al. [32]	10	5	480	F_1-score= 85.5 %
Bandyopadhyaya et al. [34]	32	90	-	Accuracy = 94.61 % (for normal subjects) Accuracy= 91.98 % (for subjects with respiratory condition)
Tracheal sounds dependent methods				
Reyes et al. [28]	13	Not used	-	Accuracy= 100 %
Huq & Moussavi [27]	93	Not Used	-	SE= 95.5%, Accuracy= 95.6%, and Specificity= 95.6 %
Kulkas et al. [5]	Not Used	6	-	SE= 98 %, PPV= 100 %, and F_1-score= 98.9 %
Chuah & Moussavi [26]	11	Not used	17	Accuracy= 93 %

subjects. Moreover, as mentioned in [33], all three methods [25, 32, 33] are computationally expensive since they utilize deep learning processes, whereas the proposed method utilizes simple signal processing steps which makes it an ideal candidate for the clinical setting where fast processing may be helpful to support clinical decision-making. Additionally, our method achieved comparable results to the envelope-based method introduced by Bandyopadhyaya et al. [34]. However, our method has been tested on a larger and more heterogeneous dataset which includes longitudinal data where lung sound or breathing patterns may change with time or disease progression. Indeed, as can be seen from Table 4, our study involves the largest number of subjects for evaluating the performance of the algorithm (125 with 10 healthy subjects and 115 respiratory disease subjects) of any other published study [25,26,5,27,28,32,33,34].

Moreover, in terms of clinical applicability, our method can be used in conjunction with methods to detect and classify crackles and wheezes without the need for additional, synchronized recording channels or additional devices. For example, we plan to integrate it with our crackle separation technique, the iterative envelope mean fractal dimension filter [38]. This integration can provide an automatic means of: i) calculating the number of crackles per breath cycle, which can be used to monitor the severity of the disease in patients with interstitial lung disorders, ii) calculating the number of crackles per inspiratory or expiratory phase, which has demonstrated potential as a novel metric for evaluating the effectiveness of breathing therapy interventions [45]; and iii) determining the timing of crackles within the breathing cycle (whether they occur during inspiration or expiration, and whether they are early. mid or late in the phase), as this information could hold clinical importance in evaluating a patient's breathing condition and in distinguishing between various cardiorespiratory disorders [25]. Integration with signal processing-based wheeze detection systems [e.g., 46] should also be feasible.

The identification of breathing phases is a difficult problem because the signals we are interested in are not just breath sounds, they may have added sounds (crackles and wheezes) and perhaps noise and movement artefacts, also. These non-breathing sounds may work to confound the automatic identification of the breath phases by, for example, making the expiratory phase louder than the inspiratory. The most challenging added sounds are crackles as the signal to noise ratio (SNR) can be high throughout a phase of the breath cycle and because they are broad-band sounds, which overlap with the frequency of the breathing sounds. Therefore, in this study, the breathing phase identification of the algorithm in the presence of crackles was tested using two datasets (IPF longitudinal and cross sectional). Additionally, the performance of the proposed algorithm was tested on a limited sample without any adventitious sounds (10 healthy subjects) and a limited sample with wheezes (41 subjects, 9 with COPD and 32 with asthma) [36].

Although the method showed good results in terms of identifying the breathing phases, it has several limitations. First, as noted in [47], the Savitzky–Golay (SG) filter provides poor noise suppression at frequencies above the cutoff. This limitation of the SG filter, combined with the non-adaptive SG filter parameters used in this study, may result masking of the inspiratory and expiratory phases in the second derivative of the input signal, especially in the presence of high-frequency noise. In future research, lung sound denoising techniques (e.g., [48, 49]) could be added as an additional pre-processing step in the proposed algorithm if needed. Additionally, there is potential for further improvement by exploring automated methods for selecting SG filter parameters based on the characteristics of the lung sounds dataset. Second, the method has a dependency on the selection of the cut-off frequency of the low pass filter, which is not adaptive to the data. It is important to notice that

in our analysis we used two different user-selected cut-off frequencies. A subject with cardiorespiratory disease generally breathes faster than a healthy subject therefore a 2.5 Hz cut-off frequency was used for the IPF longitudinal, cross-sectional, and open access datasets, and a 1 Hz cut-off frequency was used for the healthy subject longitudinal dataset. The higher cut-off frequency may generate too many false peaks and valleys which increases the chance of identifying too many breathing phases. On the other hand, the lower cut-off frequency may smooth out the true peaks and valleys of the breathing phases (especially in the case of fast breathing) which may increase the chances of under-identification. A facility for automatic selection of the low pass filter cut-off frequency according to the breathing pattern is an area for further exploration. Third, this study did not explore the effect of lung sound recording devices on the performance of the proposed algorithm, since all three of our datasets (IPF longitudinal dataset, Healthy subject longitudinal dataset, and Cross-sectional dataset), as well as the open-access dataset, were recorded using the 3M Littmann Electronic stethoscope (model 3200). As highlighted in [50], different recording devices use different acquisition preprocessing. Moreover, different recording devices may generate different levels of signal distortion in lung sounds. Therefore, future evaluation of the algorithm on lung sounds recorded from a range of recording devices would provide valuable insights into the generalizability of the algorithm across different hardware platforms. Fourth, the algorithm was evaluated against an audio-visual assessment made by a single pulmonary acoustics researcher. As mentioned by Pinho et al. [51], human assessment is associated with high levels of subjectivity. Therefore, future research should consider comparing the performance of the algorithm against a multi-annotator' gold standard.

We note also that when selecting test samples for the study, 16 % of healthy subject files, 14 % of IPF cross-section files and 17 % of open access database files were excluded prior to the analysis due to complete inaudibility of the breathing sounds, which meant that the audio-visual mark-up could not be carried out. These very quiet recordings may be due to lack of subject compliance with the instruction to breathe deeply, poor stethoscope-subject contact, or subject's body morphology, but absence of breath sounds can also be related to pathologies such as airway obstruction, hyperinflation, pneumothorax or pleural effusion. This highlights the importance of recording quality and suggests that for a system in clinical use, an important aspect of functionality would be real time assessment of recording quality.

6. Conclusions

This work presented a novel method for breathing phase identification in recorded lung sounds. Key points of the study were: (1) the method was tested on a large, heterogeneous data set of real lung sounds (1263 recordings) recorded from 125 subjects (with and without respiratory disease) at different chest locations including recordings with both crackles and wheezes; (2) the method showed very good and well-balanced performance, with SE (92.51 (12.93) %), PPV (91.09 (15.42) %), and F_1-score (90.78 (12.37)%); (3) the method utilizes fast, time domain signal processing steps that make it computationally efficient compared to recently published deep learning methods; (4) the method is applicable to recordings made directly on the chest wall with no requirement for simultaneous recording of tracheal sounds; The method automatically classifies the breathing phases within a recording, which can help clinicians when using recordings to diagnose or monitor disease. Future research will (1) seek to automate the low pass filtering threshold based on the initial breath phase identification outputs, (2) explore the performance of the method on a yet more diverse dataset to be recorded at different clinical settings from different age populations (children, young adults, older people) with a wider range of cardiorespiratory diseases to evaluate its ability to identify breathing phases in different breathing patterns and (3) test the validity of the algorithm to detect the beginning and end of each breath phase and hence its potential for measuring breath phase duration.

Acknowledgments

This work was supported by the NIHR Southampton Biomedical Research Centre, the Engineering and Physical Sciences Research Council (EPSRC), and 1he AAIR Charity.

Declaration of Competing Interest

None declared.

References

[1] R. Palaniappan, K. Sundaraj, S. Sundaraj, N. Huliraj, S.S. Revadi, A novel ap- proach to detect respiratory phases from pulmonary acoustic signals using normalised power spectral density and fuzzy inference system, Clin. Respir. J. 10 (2016) 486–494.

[2] P. Hult , T. Fjällbrant , B. Wranne , O. Engdahl , P. Ask , An improved bioacoustic method for monitoring of respiration, Technol. Health Care 12 (4) (2004) 323–332.

[3] M. Folke, L. Cernerud, M. Ekstrom, B. Hok, Critical review of non-invasive respiratory monitoring in medical care, Med. Biol. Eng. Comput. 41(4) (2003) 377–383.

[4] R. Palaniappan, K. Sundaraj, S. Sundaraj, Adaptive neuro-fuzzy inference system for breath phase detection and breath cycle segmentation, Comput. Methods Progr. Biomed. 145 (2017) 67-72.

[5] A. Kulkas, E. Huupponen, J. Virkkala, M. Tenhunen, A. Saastamoinen, E. Rauhala, S.-L. Himanen, Intelligent methods for identifying respiratory cycle phases from tracheal sound signal during sleep, Computers in Biology and Medicine 39 (2009) 1000 – 1005.

[6] S. So, D. Jain, N. Kanayama, Piezoelectric sensor-based continuous monitoring of respiratory rate during sleep, J. Med. Bio. Eng. 41 (2021) 241-250.

[7] A. Rasheed, E. Iranmanesh, W. Li, Y. Xu, Q. Zhou, H. Ou, K. Wang, An Active Self-Driven Piezoelectric Sensor Enabling Real-Time Respiration Monitoring, Sensors 19 (2019) 3241.

[8] B.Islam, MM. Rehman, T. Ahmed, M. Y. Ahmed, MM. Hasan, V. Nathan, K. Vatanparvar, E. Nemati, J. Kuang, J. A. Gao, Breath track: detecting regular breathing phases from unannotated acoustic data captured by a smartphone, Proc. ACM Interact. Mob. Wearable Ubiquitous Technol. 5 (3):124 (2021) 1-22.

[9] AMA Digital health care study, 2022.

[10] A. Marques, A. Bruton, A. Barney, The reliability of lung crackle characteristics in cystic fibrosis and bronchiectasis patients in a clinical setting, Physiological Measurement 30 (2009) 903–912.

[11] B. Zimmerman, D. Williams, Lung Sounds, In: StatPearls [Internet] (2019).

[12] D. Bardou, K. Zhang, S. M.Ahmad, Lung sounds classification using convolutional neural networks, Artificial Intelligence in Medicine 88 (2018) 58-69.

[13] M. Kompis, H. Pasterkamp, G. R. Wodicka, Acoustic Imaging of the Human Chest, Chest 120 (2001) 1309-1321.

[14] K. Douros, V. Grammeniatis, I. Loukou, Crcakles and other lung sounds, In Breath Sounds; Springer International Publishing: Cham, Switzerland 12 (2018) 225-236.

[15] A. Marques, A. Oliveira, Normal Versus Adventitious respiratory Sounds, In Breath Sounds; Springer International Publishing: Cham, Switzerland 10 (2018) 181-206.

[16] B. M. Rocha, D. Pessoa, A. Marques, P. Carvolho, R. P. Paiva, Automatic Classification of Adventitious Respiratory Sounds: A (Un)Solved Problem?, Sensors, 21(1):57 (2021).

[17] C. S. Shim, M. H. Williams, Relationship of Wheezing to the Severity of Obstruction in Asthma, Arch Intern Med 143 (1983) 890-892.

[18] R. Naves, B. H. G. Barbosa, D. D. Ferreira, Classification of lung sounds using higher-order statistics: A divide-and-conquer approach, Computer Methods and Programs in Biomedicine 129 (2016) 12-20.

[19] R. X. A. Pramono, S. Bowyer, E. Rodriguez-Villegas, Automatic adventitious respiratory sound analysis: A systematic review, PLoS ONE 12 (5) (2017) 1-43.

[20] A. R. A. Sovijarvi, L.P. Malmberg, G. Charbonneau, J. Vanderschoot, F. Dalmasso, C. Sacco, M. Rossi, J.E. Earis, Characteristics of breath sounds and adventitious respiratory sounds, Eur. Respir. Rev. 10 (77) (2000) 591–596.

[21] G. R. Epler, C. B. Carrington, E. A. Gaensler, Crackles (rales) in the interstitial pulmonary diseases, Chest 73 (3) (1978) 333-339.

[22] N. Meslier, G. Charbonneau, JL Racineux, Wheezes, European Respiratory Journal 8 (11) (1995) 1942-1948.

[23] A. Gurung, C. G. Scrafford, J. M. Tielsch, O. S. Levine, W. Checkley, Computerized lung sound analysis as diagnostic aid for the detection of abnormal lung sounds: A systematic review and meta-analysis, Respiratory Medicine 105 (9) (2011) 1396–1403.

[24] S. C. Tarrant, R. E. Ellis, F. C. Flack, W. G. Selley, Comparative Review of Techniques for Recording Respiratory Events at Rest and during Deglutition, Dysphagia, 12 (1997) 24–38.

[25] C. Jacome, J. Ravn, E. Holsbo, J. C. Aviles-Solis, H. Melbye, L. A. Bongo, Convolutional Neural Network for Breathing Phase Detection in Lung Sounds, Sensors 19 (2019) 1798.

[26] J. S. Chuah, Z. K. Moussavi, Automated Respiratory Phase Detection by Acoustical Means, In Proc. Systems, Cybernetics & Informatics (SCI) Conf. (2000) 228–231.

[27] S. Huq, Z. Moussavi, Acoustic breath-phase detection using tracheal breath sounds. Med. Biol. Eng. Comput. 50 (2012) 297–308.

[28] B. A. Reyes, N. Reljin, Y. Kong, Y. Nam, S. Ha, K. H. Chon, Towards the Development of a Mobile Phonopneumogram: Automatic Breath-Phase Classification Using Smartphones. Annals of Biomedical Engineering 44 (9) (2016) 2746–2759.

[29] A. Bohadana, G. Izbicki, S. S. Kraman, Fundamentals of Lung Auscultation, New England Journal of Medicine 370 (8) (2014) 744-751.

[30] D. Dellweg, P. Haidl, K. Siemon, P. Appelhans, D. Kohler, Impact of breathing pattern on work of breathing in healthy subjects and patients with COPD, Respiratory Physiology & Neurobiology 161 (2008) 197–200.

[31] S. Todd, E. S. Walsted, L. Grillo, R. Livingston, A. Menzies-Gow, J. H. Hull, Novel assessment tool to detect breathing pattern disorder in patients with refractory asthma, Respirology 23 (2018) 284–290.

[32] E. Messner, M. Fediuk, P. Swatek, S. Scheidl, Freyja-Maria Smolle-Juttner, H. Olschewski, F. Pernkopf, Crackle and Breathing Phase Detection in Lung Sounds with Deep Bidirectional Gated Recurrent Neural Networks, in Proc.40th Annu. Int. Conf. IEEE Eng. Med. Biol. Soc. (2018) 356–359.

[33] I. Mclane, E. Lauwers, T. Stas, I. Busch-Vishniac, K. Ides, S. Verhulst, J. Steckel, Comprehensive Analysis System for Automated Respiratory Cycle Segmentation and Crackle Peak Detection, IEEE Journal of Biomedical and Health Informatics 26 (4) (2022) 1847-1860.

[34] I. Bandyopadhyaya, M. A. Islam, P. Bhattacharyya, G. Saha, Automatic lung sound cycle extraction from single and multichannel acoustic recordings, Biomedical Signal Processing and Control 64 (2021) 102332.

[35] M. N. M. Salleh, N. Talpur, K. Hussain, Adaptive neuro-fuzzy inference system: overview, strengths, limitations, and solutions, in: Proceedings of the DMBD (2017) 527-535.

[36] M. Fraiwan, L. Fraiwan, B. Khassawneh, A. Ibnian, A dataset of lung sounds recorded from the chest wall using an electronic stethoscope, Data in Brief 35 (2021) 106913.

[37] A. Savitzky, M. J. E. Golay, Smoothing and Differentiation of Data by Simplified Least Squares Procedures. Anal. Chem. 36 (8) (1964) 1627–1639.

[38] R. Pal, A. Barney, Iterative envelope mean fractal dimension filter for the separation of crackles from normal breath sounds, Biomedical Signal Processing and Control 66 (2021) 102454.

[39] L. Vannuccini, M. Rossi, G. Pasquali, A new method to detect crackles in respiratory sounds, Technol. Health Care 6 (1) (1998) 75-79.

[40] R. Pal, A novel method for automatic separation of pulmonary crackles from normal breath sounds, University of Southampton (2021).

[41] M. Kompis, H. Pasterkamp, Y. Oh, G. R. Wodicka, Distribution of inspiratory and expiratory respiratory, In Proceedings - 19th International Conference - IEEE/EMBS (1997) 2047–2050.

[42] Z. K. Moussavi, M. T. Leopando, G. R. Rempe, Automated detection of respiratory phases by acoustical means. In Proceedings of the 20th Annual International Conference of the IEEE Engineering in Medicine and Biology Society 20 (1) (1998) 21–24.

[43] G. Sgalla, Characterization of lung sounds for early identification and monitoring of fibrotic Interstitial Lung Disease, University of Southampton (2017).

[44] B. J. Erickson, F. Kitamura, Magician's Corner: 9. Performance Metrics for Machine Learning Models, Radiology: Artificial Intelligence 3(3) (2021) e200126.

[45] A. Marques, A. Bruton, A. Barney, A. Hall, Are crackles an appropriate outcome measure for airway clearance therapy?, Respir. Care 57 (9) (2012) 1468-1475.

[46] C. Habukawa, N. Ohgami, N. Matsumoto, K. Hashino, K. Asai, T. Sato, and K. Murakami, A wheeze recognition algorithm for practical implementation in children, PLoS ONE 15(10): e0240048 (2020).

[47] M. Schmid, D. Rath, U. Diebold, Why and How Savitzky-Golay Filters Should Be Replaced, ACS Meas. Sci. Au 2 (2022) 185−196.

[48] M.F. Pouyani, M. Vali, M.A. Ghasemi, Lung sound signal denoising using discrete wavelet transform and artificial neural network, Biomed. Signal Process. Control 72 (2022), 103329.

[49] N.S. Haider, A.K. Behera, Respiratory sound denoising using sparsity-assisted signal smoothing algorithm, Biocybernet. Biomed. Eng. 42 (2) (2022) 481–493.

[50] S. E. Pajoy, J. P. Ugarte, Computerized analysis of pulmonary sounds using uniform manifold projection, Chaos, Solitons and Fractals 166 (2023) 112930.

[51] C. Pinho, A. Oliveira, C. Jacome, J. Rodrigues, A. Marques, Automatic Crackle Detection Algorithm Based on Fractal Dimension and Box Filtering. Procedia Computer Science 64 (2015) 705–712.